

- Zone of Ladakh* (eds Thakur, V. C. and Sharma, K. K.), Wadia Institute of Himalayan Geology, Dehradun, 1983, pp. 79–91.
25. Krogh, T. E., Improved accuracy of U–Pb zircon ages by the creation of more concordant systems using the air abrasion technique. *Geochim. Cosmochim. Acta*, 1982, **46**, 637–649.
 26. Stacey, J. S. and Kramers, J. D., Approximation of terrestrial lead isotope evolution by a two stage model. *Earth Planet. Sci. Lett.*, 1975, **127**, 30–45.
 27. Ludwig, K. R., PBDAT for MS-DOS: a computer program for IBM-PC compatibles for processing raw Pb–U–Th isotope data. *US Geol. Survey Open-File Rep.*, 1988, 88–0542.
 28. Ludwig, K. R., Isoplot 3.00 – a geochronological toolkit for Microsoft Excel. *Berkeley Geochronol. Center Spl. Publ.*, 2003, 4.
 29. Upadhyay, R., Implications of U–Pb zircon age of the Tirit granitoids on the closure of the Shyok suture zone, northern Ladakh, India. *Curr. Sci.*, 2008, **94**, 1635–1640.
 30. Treloar, P. J., Petterson, M. G., Jan, Q. M. and Sullivan, M. A., A re-evaluation of the stratigraphy and evolution of the Kohistan arc sequence, Pakistan Himalaya: implications for magmatic and tectonic arc-building processes. *J. Geol. Soc. London*, 1996, **153**, 681–693.
 31. Honegger, K., Dietrich, V., Frank, W., Gansser, A., Thoni, M. and Trommsdorff, V., Magmatism and metamorphism in the Ladakh Himalayas, the Indus Tsangpo suture zone. *Earth Planet. Sci. Lett.*, 1982, **60**, 253–292.
 32. Schärer, U., Xu, R. H. and Allegre, C. J., U–Pb geochronology of Gangdese, trans-Himalaya, plutonism in the Lhasa–Xigaze region, Tibet. *Earth Planet. Sci. Lett.*, 1984, **69**, 311–320.
 33. Weinberg, R. F. and Dunlap, W. J., Growth and deformation of the Ladakh Batholith, northwest Himalayas: implications for timing of continental collision and origin of calc-alkaline batholith. *J. Geol.*, 2000, **108**, 303–320.
 34. Upadhyay, R., Frisch, W. and Siebel, W., Tectonic implications of new U–Pb zircon ages of the Ladakh batholith, Indus suture zone, northwest Himalaya, India. *Terra Nova*, 2008, **20**, 309–317.
 35. George, M. T., Harris, N. B. W. and Butler, R. W. H., The tectonic implications of contrasting granite magmatism between Kohistan island arc and the Nanga Parbat–Haramosh massif, Pakistan Himalaya. *Geol. Soc. London Spl. Publ.*, 1993, **74**, 173–191.
 36. Searle, M. P., Crawford, M. B. and Rex, A. J., Field relations, geochemistry, origin and emplacement of the Baltoro granite, Central Karakoram. *Trans. R. Soc. Edinburgh Earth Sci.*, 1992, **83**, 519–538.
 37. Searle, M. P., Parrish, R. R., Tirrul, R. and Rex, D. C., Age of crystallization and cooling of the K2 gneiss in the Baltoro Karakoram. *J. Geol. Soc. London*, 1990, **147**, 603–606.
 38. Phillips, R. J., Parrish, R. R. and Searle, M. P., Age constraints on ductile deformation and long-term slip rates along the Karakoram fault zone, Ladakh. *Earth Planet. Sci. Lett.*, 2004, **226**, 305–319.
 39. Searle, M. P. and Phillips, R. J., Relationships between right-lateral shear along the Karakoram fault and metamorphism, magmatism, exhumation and uplift: evidence from the K2–Gasherbrum–Pangong ranges, North Pakistan and Ladakh. *Geol. Soc. London*, 2007, **164**, 439–450.
 40. Lacassin, R. *et al.*, Large scale geometry, offset and kinematic evolution of the Karakoram fault, Tibet. *Earth Planet. Sci. Lett.*, 2004, **219**, 255–269.
 41. Searle, M. P., Parrish, R. R., Hodges, K. V., Hurford, A., Ayres, M. W. and Whitehouse, M. J., Shisha Pangma leucogranite, south Tibetan Himalaya: field relations, geochemistry, age, origin and emplacement. *J. Geol.*, 1997, **105**, 295–317.
 42. Burg, J. P., Brunel, M., Gapais, D., Chen, G. M. and Liu, G. H., Deformation of leucogranites of the crystalline Main Central Thrust sheet in southern Tibet (China). *J. Struct. Geol.*, 1984, **6**, 535–542.
 43. Royden, L. and Burchfiel, B. C., Thin-skinned N–S extension within the convergent Himalayan region: Gravitational collapse of a Miocene topographic front. *Geol. Soc. London Spl. Publ.*, 1987, **28**, 611–619.
 44. Parrish, R. R. and Tirrul, R., U–Pb age of the Baltoro granite, northwest Himalaya, and implications for monazite U–Pb systematics. *Geology*, 1989, **17**, 1076–1079.

ACKNOWLEDGEMENTS. I thank Profs W. Frisch and W. Siebel for providing facilities for research at the Institute of Geosciences, University of Tuebingen, Germany. I also thank the Alexander von Humboldt Foundation, Germany for providing AvH Fellowship (2003–04). I also thank Dr Heinrich Taubald and Mrs Gisela Bartholoma for their help in geochemical data generation; the Director, BSIP, Lucknow for organizing a geological field excursion in Ladakh during 2002 and the Head, Department of Geology, Kumaun University, Nainital for providing facilities for research within the framework of UGC-SAP and DST-FIST programmes.

Received 18 December 2008; revised accepted 14 August 2009

Evidences for seawater–rock hydrothermal interaction in the serpentinites from Northern Central Indian Ridge

Dwijesh Ray^{1*}, Ranadip Banerjee², Sridhar D. Iyer² and Subir Mukhopadhyay³

¹National Centre for Antarctic and Ocean Research, Vasco-da-Gama, Goa 403 804, India

²Geological Oceanography, National Institute of Oceanography (CSIR), Goa 403 004, India

³Department of Geological Sciences, Jadavpur University, Kolkata 700 032, India

Serpentinites and serpentinitized harzburgites were collected from a ridge-transform intersection at 6°39'S–68°19'E from the Northern Central Indian Ridge. The degree of serpentinitization is extensive and varies from 90 to 100%. Olivine and orthopyroxene are largely pseudomorphed to lizardite-chrysotile 'mesh' and 'bastite' respectively. Numerous serpentine vein network associated with clusters of magnetite are also present. On the basis of mineralogical paragenesis, mineral chemistry and bulk rock analyses, we infer that the present serpentinites might have formed due to the interaction of harzburgites and seawater at a low temperature. Additionally, positive Eu anomaly, higher La/Sm and low Nb/La ratios suggest substantial hydrothermal input during the onset of serpentinitization.

Keywords: Hydrothermal alteration, mid-oceanic ridge, Northern Central Indian Ridge, serpentinites, seawater–rock interaction.

THE Northern Central Indian Ridge (NCIR; half spreading rate of 18–22 mm/year), one of the least explored

*For correspondence. (e-mail: dwijesh@rediffmail.com)

ocean ridge systems is an important locale to examine the chemistry of the juvenile Indian Ocean crust and nature of the underlying mantle. Limited petrological work has been carried out along NCIR^{1,2}. The nature of interaction between peridotite and seawater is relatively unknown along NCIR as compared to the Mid-Atlantic Ridge (MAR) and the East Pacific Rise (EPR)^{3,4}. Serpentinities are commonly thought to represent hydrated mantle peridotite and generally have a tendency to be exposed at rift valley, transform fault or at detachment fault zones. Till date, the chemical conditions and style of hydrothermal alteration of the oceanic lithosphere along segments of the Indian Ocean ridges are poorly understood. Serpentinization processes also play a crucial role on ocean biogeochemistry and conditions of emergence of life on earth. The present communication is aimed at presenting a few important findings on the geochemistry of serpentinites and serpentinized harzburgites, recovered from the NCIR (at 6°39'S/68°19'E; water depth 2800 m). Their evolution due to the possible effect of low temperature seawater–peridotite interaction (hydrothermal alteration) is also discussed.

In hand specimen, the present serpentinites appear to be mostly greyish to dark greenish in colour, medium to coarse-grained and have interlocking textures. Features like foliation with a shear plane, lineation marks (slickenside) and remnants of serpentine patches are also common. Morphologically, serpentines are platy or flaky in habit, often fibrous, with a soapy texture and mostly composed of chrysotile and lizardite. X-ray diffraction (XRD) results of bulk serpentinite (Figure 1) reveal distinct peaks for both chrysotile and lizardite, more specifically 1T-lizardite (PDF No. 11-386), 2M chrysotile (PDF No. 31-808), and orthochrysotile (PDF No. 25-645) (ref. 5). Serpentine veins and veinlets occur in a criss-cross pattern, are often lensoidal or even exhibit 'pinch' and 'swell' structures. Different generations of veins can be deciphered from their cross-cut relationship. 'Mesh' (pseudomorph after olivine) and 'bastite' (pseudomorph after orthopyroxene) are the most common textures within the present serpentinites (Figure 2a and b). Spinel, the only primary mineral, occurs mostly as anhedral, irregular rounded and vermicular aggregates. Magnetite is generally precipitated during alteration of olivine and orthopyroxenes and commonly occur either perpendicular to the vein walls or as clusters outlining the altered primary phases. Apparently, the degree of serpentinization attained is up to 100% and the process took place at a new tectonic setting of ridge-transform fault intersection at NCIR.

On the basis of mineralogy (high Mg lizardite–chrysotile) and bulk rock chemistry (high MgO content), the present serpentinites indicate that they have formed due to the prolonged interaction of seawater with harzburgite. Additionally, low Al₂O₃ and TiO₂ contents support a residual nature of these NCIR harzburgites. Major oxides of serpentinites from different ridge segments of

the Indian Ocean ridge system and those from the MAR are compared in Table 1 (refs 6–9). The NCIR serpentinites have high MgO (44.21), low Al₂O₃ (0.79) and CaO (0.31) contents, as compared to the previously reported Mg sepiolite from Carlsberg Ridge (CR), lherzolites from CIR and serpentinized harzburgites from South West Indian Ridge (SWIR). Their high bulk Ni content (up to 2300 ppm) and Cr content (up to 2234 ppm) can be attributed to the higher abundance of olivine and Cr-spinel in parent peridotite. Very low concentration (<10 ppm) of the high field strength (HFS) elements (e.g. Y and Zr) in these serpentinites indicate possibility of highly acidic nature of the hydrothermal fluid that interacted with the serpentinites^{9,10}. Alternatively, the possibility of low Y and Zr content of the parent rock is also not ruled out. The low Ba content (6–28 ppm) in the bulk rock could be due to sub-seafloor barite precipitation from the interacting hydrothermal fluid. The possibility of Ba getting mobilized out of the parent rock during rock-hydrothermal fluid interaction is also not ruled out, which is in accord with the serpentinite composition and Ba decreases as the degree of serpentinization increases.

In the primitive mantle (PM) normalized multielement plot, the present serpentinites display enrichment of LIL elements and depletion of HFS elements (Figure 3). The distinct enrichment of U in present serpentinite appears to be correlated with low temperature alteration. Increased U content is also reported from oxidatively altered rocks from ODP Leg 504B and seawater-altered basalts^{12,13}. Most of the present samples characteristically show a moderate to strong positive Eu anomaly in chondrite-normalized rare earth elements (REE) diagram (Eu/Eu* up to +3.4, Figure 4). The total REE (Σ REE) of the present serpentinites is variable (0.7–10.8 ppm). Samples with positive Eu anomaly also display low Σ REE content (1.09–1.35). A comparison of the NCIR serpentinites with the normalized REE pattern of known ultramafic hosted hydrothermal fluid (Figure 4) demonstrates that positive Eu anomaly is common to all. The Nb/La ratio also varies from 1.44 to 3.69. Positive Eu anomaly of the NCIR serpentinites cannot be solely attributed to the plagioclase accumulation as no relict plagioclase is found

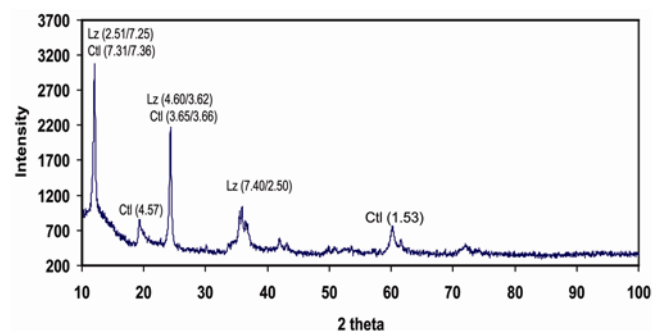


Figure 1. X-ray diffractogram of whole-rock serpentinite (Ctl, chrysotile; Lz, lizardite). D spacing of Lizardite 1T, Lizardite aluminous, 2 M clinochrysotile and orthochrysotile mentioned within the parenthesis.

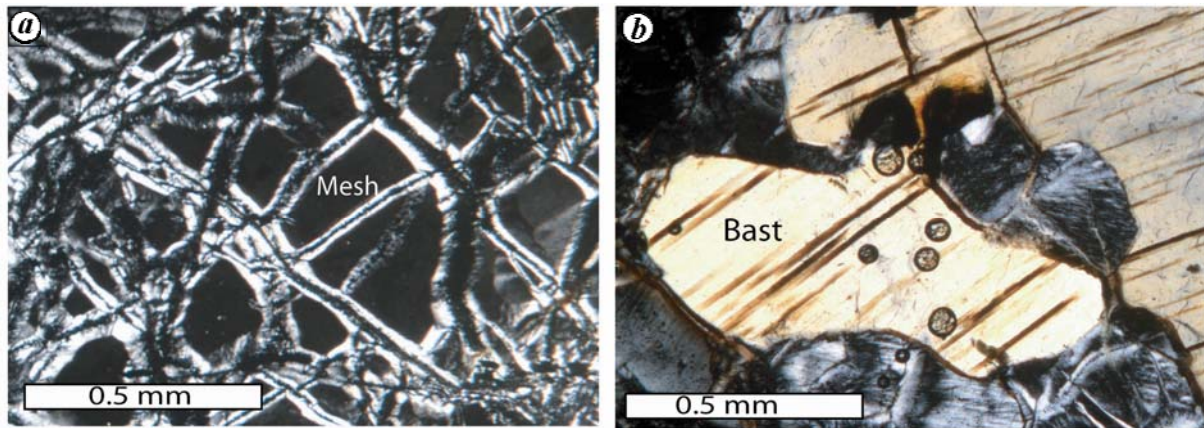


Figure 2. Photomicrographs of NCIR serpentinites. *a.* 'Mesh' texture after olivine. *b.* 'Bastite' (Bast) after orthopyroxene.

Table 1. Comparison of average major oxides of serpentinites from different locations of the world's Mid-Ocean Ridge System. Abbreviated locations are same as in text

Rock type	Indian Ocean				Atlantic Ocean MAR ⁹ Harzburgite and Dunite
	Present study NCIR (6°39'S–68°19'E) Harzburgite	CIR ⁶ (17°03'S/66°52'E) Lherzolitite	CR ⁷ (11°44'N/57°43'E) Sepiolite	SWIR ⁸ (30°S/62°E) Serpentinized peridotite	
Oxides (wt%)	<i>N</i> = 18	1	2	8	15
SiO ₂	35.83	44.15	51.95	36.72	38.84
TiO ₂	0.03	0.03	0.06	0.07	0.01
Al ₂ O ₃	0.79	3.59	1.00	9.41	0.63
FeO _t	10.05	6.67	4.85	7.74	6.89
MnO	0.17	0.10	0.23	0.16	0.1
MgO	44.21	34.84	19.00	30.64	39.42
CaO	0.31	5.50	0.89	1.00	0.24
Na ₂ O	0.15	0.19	1.05	0.56	0.1
K ₂ O	0.02	<0.01	0.55	0.09	0.01
P ₂ O ₅	0.03	n.a.	n.a.	0.04	0.01

n.a., not available; *N*, no. of samples; Total Fe as FeO_t.

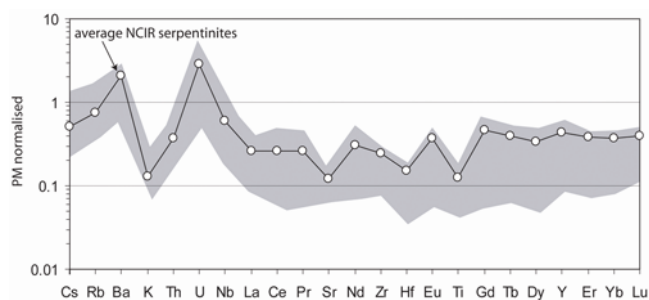


Figure 3. Primitive mantle (PM) normalized multielement spidergram of NCIR serpentinites. Average data shown in foreground and range as shown in the background. PM data taken from Sun and McDonough¹⁹.

(mostly residual in nature) in these rocks and also their bulk Sr content is very low. The enrichment of Eu over other REEs probably was generated during pronounced interaction between hydrothermal solution and ultramafic

rocks. The observed positive Eu anomaly is in good agreement with the REE content of hydrothermal fluid collected from different locales at MAR, suggesting substantial hydrothermal input during the formation processes of the NCIR serpentinites (Figure 4). A possible interaction of Eu-enriched hydrothermal fluids with the present serpentinites could have prompted an increase in the absolute Eu content in these rocks¹¹. Additionally, low Nb/La ratio (range: 1.13–3.69, avg. 1.81), in association with the highest positive Eu anomaly suggests the possibility of a higher degree of hydrothermal input and this is further supported by their higher La/Sm values (e.g. up to 4.40). Similar low Nb/La ratio is also noticed within the hydrothermal amphibole from oceanic gabbro¹⁴.

The high abundances of chrysotile and lizardite also bear some temperature constraints on formation of present serpentinites. Oxygen and hydrogen isotope ratio of serpentinites have been frequently used to establish a range of temperatures¹⁵ (e.g. temperature range for oceanic

lizardite and chrysotile are estimated as 130°C to 185°C respectively). Thus, our present mineralogical assemblages (mostly chrysotile and lizardite) also indicate a lower temperature for their formation and their paragenetic association also suggests a tendency to become stable under a similar temperature range. Serpentine mineralogy, e.g. mainly co-existence of lizardite and chrysotile favour prolonged low temperature (~250°C) alteration. Further, it suggests that the process of serpentinization in the study area was probably initiated at a low temperature and at a low to moderate pressure (generally <2 kb; ref. 16). The water-rock mass ratio is also another useful constraint during serpentinization process. Wenner and Taylor¹⁵ have estimated that the formation of lizardite and chrysotile is facilitated at water/rock mass ratio >2. The high water content (LOI > 10wt%) of the NCIR serpentinites is consistent with their mineralogy and, therefore, suggest the ongoing seawater-peridotite interaction at high water-rock ratio. The distribution of magnetite also varies with the degree of serpentinization. Abundant cross cutting magnetite veins suggest that prolonged serpentinization process might have been facilitated due to upliftment of the oceanic crust, as deformation and hydration processes are closely linked to each other. This pervasive serpentinization favours formation of extensive mesh texture, characterized by structureless serpentine replacing olivine, and pseudomorphs of lizardite in addition to the formation of orthopyroxene 'bastite' texture (Figure 2). And finally, late-formed magnetite strings along with obliteration of original textures indicate a higher degree of serpentinization.

Thus, the present serpentinites with numerous serpentine veins and variable morphologies suggest that intense alteration has taken place during a prolonged period of rock-seawater interaction at a low temperature. In addition, abundant cross-cutting veins might have resulted due to the late tectonic upliftment of the mantle peridotite, which facilitated accommodation of the opening of

vein space and subsequently filled up by chrysotiles. This is very similar to the MARK serpentinites reported from MAR¹⁷. Such an environment always creates pathways for the circulation of high temperature fluid and its subsequent migration through numerous veins. This is also exemplified by the presence of chrysotile veinlets post-dating the early serpentine veins. The occurrence of serpentinites and serpentinized harzburgites at NCIR suggests definite hydrothermal discharge and its subsequent interaction with the peridotites at a transform fault setting which is similar to the other known ultramafic-hosted hydrothermal fields, e.g. Rainbow and Logatchev at MAR^{10,18}. Additional study in the near future is required to trace the exact hydrothermal discharge zone, and also to better understand the alteration style of the NCIR upper mantle rocks.

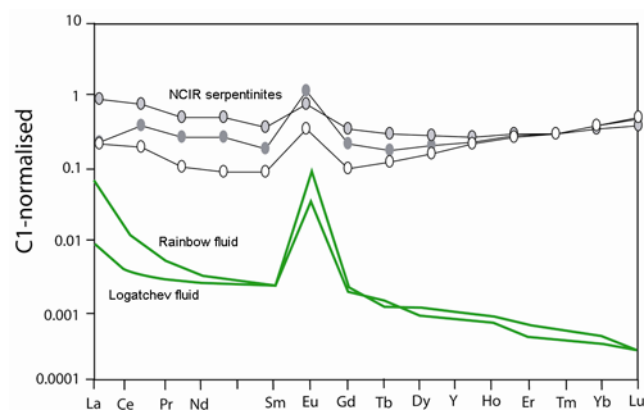


Figure 4. Representative chondrite normalized REE patterns of NCIR serpentinites and ultramafic hosted hydrothermal fluid (Logatchev and Rainbow hydrothermal fluid data taken from Douville *et al.*¹⁸).

1. Rehkamper, M. and Hoffman, A., Recycled ocean crust and sediment in Indian Ocean MORB. *Earth Planet. Sci. Lett.*, 1997, **147**, 93–106.
2. Ray, D., Iyer, S. D., Banerjee, R., Misra, S. and Widdowson, M., A petrogenetic model of basalts from the Northern Central Indian Ridge: 3–11°S. *Acta Geol. Sin.* (English Edition), 2007, **81**, 99–112.
3. Cannat, M. *et al.*, Thin crust, ultramafic exposure and rugged faulting patterns at the Mid-Atlantic Ridge (22–24°N). *Geology*, 1995, **23**, 49–52.
4. Gillis, K. M. *et al.*, Shipboard Scientific Party, Site 894, *Proc. ODP, Init. Repts.*, Ocean Drilling Program, College Station, Texas, USA, 1993, **147**, pp. 45–108.
5. Whittaker, E. J. W. and Zussman, J., The characterization of serpentine minerals by X-ray diffraction. *Mineral Mag.*, 1956, **233**, 107–126.
6. Engel, C. G. and Fisher, R. L., Granitic to ultramafic rock complexes of the Indian ocean Ridge System, western Indian Ocean. *Bull. Geol. Soc. Am.*, 1975, **86**, 1553–1578.
7. Bonatti, E., Simmons, E. C., Breger, D., Hamlyn, P. R. and Lawrence, J., Ultramafic rock/seawater interaction in the oceanic crust: Mg silicate (sepiolite) deposit from the Indian Ocean floor. *Earth Planet. Sci. Lett.*, 1983, **62**, 229–238.
8. Bassias, Y. and Triboulet, C., Petrology and P-T-t evolution of the South West Indian Ridge peridotites, A case study: east of Melville fracture zone at 62°E. *Lithos*, 1992, **28**, 1–19.
9. Paulick, H., Bach, W., Godard, M., De Hoog, J. C. M., Suhr, G. and Harvey, J., Geochemistry of abyssal peridotites (Mid-Atlantic Ridge, 15°20'N, ODP Leg 209): implication for fluid/rock interaction in slow spreading environments. *Chem. Geol.*, 2006, **234**, 179–210.
10. Douville, E., Bienvenu, P., Charlou, J., Donval, J., Fouquet, Y., Appriou, P. and Gamo, T., Yttrium and rare earth elements in fluids from various deep-sea hydrothermal systems. *Geochim. Cosmochim. Acta*, 1999, **63**, 627–643.
11. German, C. R., Hergt, J., Palmer, M. R. and Edmond, J. M., Geochemistry of a hydrothermal sediment core from the OBS ventfield, 21°N East Pacific Rise. *Chem. Geol.*, 1999, **155**, 65–75.
12. Bach, W., Peucker-Ehrenbrink, B., Hart, S. R. and Blusztajn, J. S., Geochemistry of hydrothermally altered oceanic crust: DSDP/ODP Hole 504B-Implications for seawater-crust exchange budgets and Sr- and Pb-isotopic evolution of the mantle. *Geochem. Geophys. Geosyst.*, 2003, **4**, 29.
13. Verma, S. P., Seawater alteration effects on REE, K, Rb, Cs, Sr, U, Th, Pb and Sr–Nd–Pb isotope systematics of Mid-Ocean Ridge basalts. *Geochem. J.*, 1992, **26**, 159–177.

14. Coogan, L. A., Wilson, R. N., Gillis, K. M. and MacLeod, C. J., Near solidus evolution of oceanic gabbros: Insights from amphibole geochemistry. *Geochim. Cosmochim. Acta*, 2001, **65**, 4339–4357.
15. Wenner, D. B. and Taylor, H. P., Oxygen and hydrogen isotope studies of serpentinisation of ultramafic rocks. *Am. J. Sci.*, 1973, **273**, 207–239.
16. Mével, C., Serpentinisation of abyssal peridotite at mid ocean ridges. *C. R. Geoscience*, 2003, **335**, 825–852.
17. Dilek, Y., Coulton, A. and Hurst, S. D., Serpentinisation and hydrothermal veining in peridotites at site 920 in the MARK area. *Proc. of the ODP, Sci. Results*, College Station, Texas, USA, 1997, **153**, pp. 35–59.
18. Douville, E. *et al.*, The rainbow vent fluids (26°14'N, MAR): the influence of ultramafic rocks and phase separation on trace metal content in Mid-Atlantic Ridge hydrothermal fluids. *Chem. Geol.*, 2002, **184**, 37–48.
19. Sun, S. and McDonough, W. F., Chemical and isotopic systematics of oceanic basalts: implications for mantle composition and processes. In *Magmatism in the Ocean Basins* (eds Saunders, A. D. and Norry, M. J.), Geol. Soc. Spl. Publ., 1989, vol. 42, pp. 313–345.

ACKNOWLEDGEMENTS. This research is partly funded by ONR grant and CSIR Network Programme on Indian Ocean ridges. Ship time was provided by the Department of Ocean Development, New Delhi. We appreciate the help extended by the Captain and crew members onboard ORV *Sagar Kanya* and other colleagues during the sampling operations. D.R. thanks CSIR, New Delhi, for financial support in the form of a Senior Research Fellowship. We thank an anonymous reviewer for valuable suggestions. This is NIO contribution no. 4617.

Received 11 November 2008; revised accepted 8 September 2009

Catch-up growth during juvenile life can compensate for the small metamorphic size in *Euphlyctis cyanophlyctis*

N. P. Gramapurohit

Department of Zoology, University of Pune, Pune 411 007, India

Metamorphic size in amphibians with a biphasic mode of life is known to affect adult fitness. To test whether this is true of tropical anurans, influence of metamorphic size on future survival, growth rate, age and size at sexual maturation were studied in a continuously breeding tropical frog, *Euphlyctis cyanophlyctis*. In nature, intra-population size at metamorphosis (when the tail completely disappears; Gosner stage 46) varies significantly (22–30 mm in snout-vent length (SVL)). Analysis of growth rate and determination of age at first reproduction in a group of frogs reared in the outdoor enclosures revealed that rate of increase in

SVL differed between small and large frogs only initially but comparable subsequently. Rate of increase in body mass on the other hand, was comparable between the two groups from the first month onwards until the termination of the experiment. Mortality was also comparable among the two groups. There was no difference in the size and age of individuals at first reproduction. In females, the fecundity (number of eggs laid at first reproduction) was comparable between the smaller and larger group frogs. The present study revealed no significant influence of metamorphic size on adult traits in the tropical year-round breeding frog, *E. cyanophlyctis* and that the juveniles compensate for their smaller size at metamorphosis during their terrestrial life.

Keywords: Anura, *Euphlyctis cyanophlyctis*, post-metamorphic growth, sexual maturity.

IN amphibians with a complex life cycle, the aquatic larval stage is an adaptation for exploiting rich resources of temporary water bodies that are generally devoid of permanent predators including the fish and ensure rapid growth before embarking on to the terrestrial mode of life^{1–3}. Rapid growth as larvae is believed to result in a larger size at metamorphosis which, in turn, might influence post-metamorphic survival, foraging efficiency, growth rate and adult fecundity in many anuran amphibians^{4–10}. Also, large size at metamorphosis may result in large size at first reproduction in addition to aiding early attainment of sexual maturity⁶. It is well known that fecundity and female body size are correlated in anurans^{11,12}. Theoretically, optimal size at metamorphosis should maximize fitness. However, inter- and intra-population variations in the larval period and size at metamorphosis are widespread in anurans due to various factors including phenotypic plasticity and prevailing ecological conditions^{1,3,13}. For instance, factors such as temperature, larval density, resource availability, pond duration, kinship environment and predator pressure are known to affect larval period and size of metamorphs in anurans^{14–16}.

Although both field and laboratory studies have shown the variation in larval period, growth, development and size at metamorphosis for anurans^{4,13,17,18}, the adaptive significance of this variation in the metamorphic traits is demonstrated only in a few temperate anurans^{5,19}. Moreover, it is not clear whether metamorphic size directly affects the post-metamorphic growth, juvenile mortality and timing of sexual maturation or indirectly through altered efficiency in foraging, survival and predator avoidance. What influence does the size of metamorphs have on the age and size at sexual maturity is not known especially for continuously breeding tropical anurans. Hence, the present study addresses the question whether size at metamorphosis in the Indian skipper frog, *Euphlyctis cyanophlyctis* affects juvenile survival, post-

e-mail: naraharipg@unipune.ernet.in